



Dual-mode thin film bulk acoustic wave resonators for parallel sensing of temperature and mass loading

L. García-Gancedo^{a,*}, J. Pedrós^b, X.B. Zhao^{c,d}, G.M. Ashley^e, A.J. Flewitt^a,
W.I. Milne^{a,e}, C.J.B. Ford^b, J.R. Lu^c, J.K. Luo^f

^a Electrical Engineering Division, Department of Engineering, University of Cambridge, Cambridge CB3 0FA, United Kingdom

^b Cavendish Laboratory, Department of Physics, University of Cambridge, Cambridge CB3 0HE, United Kingdom

^c Biological Physics Group, School of Physics & Astronomy, University of Manchester, Manchester M13 9PL, United Kingdom

^d Department of Chemical and Biological Engineering, University of Sheffield, Sheffield S1 3JD, United Kingdom

^e Department of Information Display, Kyung Hee University, Seoul 130-701, Republic of Korea

^f Institute for Materials Research and Innovation (IMRI), University of Bolton, Bolton BL3 5AB, United Kingdom

ARTICLE INFO

Article history:

Received 5 March 2012

Received in revised form

18 May 2012

Accepted 14 June 2012

Available online 21 June 2012

Keywords:

Piezoelectric biosensor

FBAR

Zinc oxide (ZnO)

Gravimetric biosensor

ABSTRACT

Thin film bulk acoustic wave resonator (FBAR) devices supporting simultaneously multiple resonance modes have been designed for gravimetric sensing. The mechanism for dual-mode generation within a single device has been discussed, and theoretical calculations based on finite element analysis allowed the fabrication of FBARs whose resonance modes have opposite reactions to temperature changes; one of the modes exhibiting a positive frequency shift for a rise of temperature whilst the other mode exhibits a negative shift. Both modes exhibit negative frequency shift for a mass load and hence by monitoring simultaneously both modes it is possible to distinguish whether a change in the resonance frequency is due to a mass load or temperature variation (or a combination of both), avoiding false positive/negative responses in gravimetric sensing without the need of additional reference devices or complex electronics.

© 2012 Elsevier B.V. All rights reserved.

1. Introduction

Over the last decade there has been an increased interest in developing highly sensitive resonators for gravimetric sensing (Wingqvist, 2010; Lee and Song, 2010; Rey-Mermet et al., 2006). Thin film technology has been adopted as the optimum approach for the fabrication of high frequency (\sim GHz range) bulk acoustic wave (BAW) resonators, with a frequency of resonance, f_r , which is dependent on the device structure and size; and the quality of the films utilised for their fabrication. The addition of a mass on the resonator surface lowers f_r due to the increase of the thickness of the resonance cavity and to variation of the energy confinement in the sensed layer (due to acoustic impedance mismatch). The magnitude of the frequency shift, Δf_r , is a function of the additional mass. By tracking changes in f_r , mass changes on the resonators (for example due the adsorption of biological samples) can be detected, being the total mass bound on the resonator's surface proportional to the change in f_r .

The frequency shift, Δf_r , for a given mass load is proportional to the square of f_r (Sauerbrey, 1959; Gabl et al., 2004), hence

resonators working at higher frequencies, possess, in theory, a better sensitivity, as a higher Δf_r is induced for the same change in mass compared to those with lower f_r . However, higher f_r cause all environmental and boundary conditions to affect the operation of the BAW resonators more strongly than for lower f_r s. One of the most important challenges that still needs to be overcome is the frequency drift over temperature, resulting in undesirable false-positive/negative responses. The speed of propagation of acoustic waves within a material is generally dependent on the temperature, and also the thickness of the thin films will change (up to several ppm \cdot K⁻¹) due to their coefficients of thermal expansion (CTE), and hence frequency shifts of up to several kHz will occur due to a change in temperature. These frequency shifts are indistinguishable from those due to mass loading and hence sensing must be carried out in an environment where the temperature is constant, the impracticability of this being obvious. To overcome this issue, a reference device isolated from the species to be measured can be used in addition to the sensing device (Razafimandimby et al., 2006). In this scenario, Δf_r due to a mass load can be extrapolated from the Δf_r measured on the sensing device and on the reference device. Alternatively, temperature readout circuitry can be integrated with the resonator and real-time temperature compensation can be implemented via software processing (Rai et al., 2009, 2010). Either of these techniques, however, increases the cost of the sensor, its

* Corresponding author. Tel.: +44 1223 748304.

E-mail address: luis.garcia-gancedo@eng.cam.ac.uk (L. García-Gancedo).

physical size and makes the electronics much more complicated. Elimination of the temperature effects has also been attempted by designing the resonators with multi-layers of opposite temperature coefficients of frequency (TCF) that would compensate the frequency shifts due to temperature variations; however non-linearities on the material properties limit the resonator's stable behaviour range to just a few degrees celsius (Pang et al. 2008; Wingqvist et al., 2009).

In this work, thin film bulk acoustic wave resonators (FBARs) specifically designed to support multiple longitudinal resonant modes at different frequencies reacting differently to temperature and mass changes are presented. These devices allow direct and independent discrimination of frequency shifts due to mass or temperature changes, thereby eliminating the need for a reference device and complex electronics.

2. Experimental: Device design and fabrication

The devices consist of a thin film of ZnO ($\sim 2 \mu\text{m}$) deposited on a thin film of SiO_2 ($\sim 2 \mu\text{m}$), which was thermally grown on a Si (100) wafer, and sandwiched between Cr/Au electrodes as shown schematically in Fig. 1.

The fabrication process commenced with removing the SiO_2 layer on one side of the Si wafer through a reactive ion etching (RIE) process with a carbon tetrafluoride (CF_4) plasma. A thin layer ($\sim 100 \text{ nm}$) of Al_2O_3 , which acts as a hard mask on a forthcoming deep reactive ion etching (DRIE) was reactively sputtered and patterned on the SiO_2 -free side to define the membranes. The bottom electrodes (4/70 nm Cr/Au) were patterned through a standard photolithography process and thermally evaporated on the top SiO_2 layer. The ZnO piezoelectric films were then reactively sputtered from a 4-in. diameter metallic Zn target in a high target utilisation sputtering (HiTUS) system (Flewitt et al., 2009; García-Gancedo et al., 2010, 2011; Pedros et al., 2011), which provides homogeneous and repeatable ZnO thin film properties (García-Gancedo et al., 2012). The ZnO films were sputtered with a 10:7 Ar: O_2 admixture at a total pressure of $\sim 3 \times 10^{-3} \text{ mbar}$, and at room temperature. These conditions provided deposition rates of $\sim 50 \text{ nm min}^{-1}$. The thickness of the ZnO layer was set to 2000 nm.

The crystal quality of the sputtered ZnO films was assessed by X-ray diffractometry (XRD) using $\text{Cu K}\alpha$ radiation. The θ - 2θ scan of the samples over a broad angle range ($2\theta = 20^\circ$ – 80°) confirmed the high degree of orientation of the films along the (0001) or c -axis. This is shown in Fig. 2 where only the peaks corresponding to the (0002) and (0004) ZnO planes, together with those of the (100) Si planes and (111) Au planes are observed. The identification of the peaks is based on their tabulated values (ICDD Powder-Diffraction-Files). The rest of the features, labelled with a * symbol, correspond to contamination lines produced by the

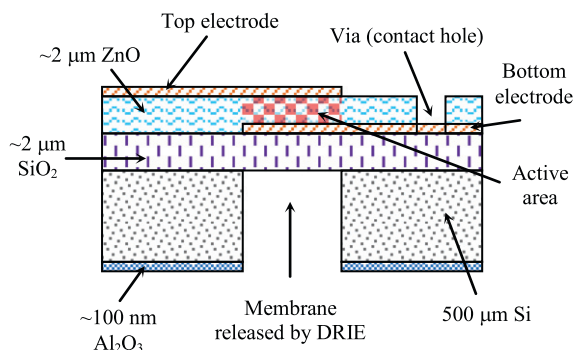


Fig. 1. Schematic view of the devices fabricated.

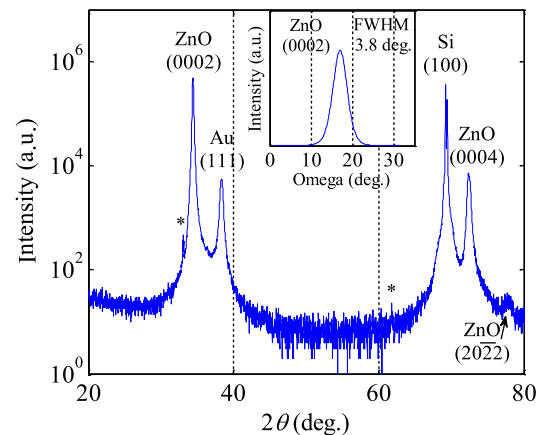


Fig. 2. X-ray diffractogram of ZnO films in a θ - 2θ configuration. The features labelled with a * symbol correspond to substrate-related peaks due to contamination lines. The inset shows the rocking curve of the ZnO (0002) peak.

filament. The inset of Fig. 2 presents the rocking curve of the most intense reflection from ZnO, i.e., the (0002) peak at $\theta = 17.4^\circ$. The peak has a full width at half maximum (FWHM) of 3.8° , indicating the small angular dispersion of the crystallites around the c -axis thereby ensuring a strong piezoelectricity.

After ZnO deposition, via etch holes were formed through the ZnO for electrical connection to the Cr/Au bottom electrode by wet etching the ZnO in a 2% glacial acetic acid and phosphoric acid solution at room temperature. The top electrode was then patterned with a lift-off photolithography process with identical materials and thicknesses to the bottom electrode. Finally the Si from the back of the wafer was removed with a deep reactive ion etching (DRIE) process to release the SiO_2/ZnO membrane.

3. Results and discussion

3.1. Device response and numerical simulations

The resonant frequencies of the FBAR devices were measured with a coplanar probe station (on a GSG configuration) connected to a network analyser, and are shown in Fig. 3a. Two fundamental modes of resonance are observed at 754 MHz (mode I hereafter) and 1.44 GHz (mode II hereafter), with their second harmonics at 2.26 GHz and 4.34 GHz respectively. The third harmonic of mode I is found at 3.77 GHz (inset of Fig. 2). The first fundamental mode (mode I) is attributed to the resonance of the SiO_2/ZnO bi-layer stack and occurs when a half wavelength equals the combined thickness of the ZnO and SiO_2 layers. The second fundamental mode (mode II) is attributed to the resonance of the ZnO layer alone and occurs when a half wavelength equals the thickness of the ZnO layer, but it is also greatly influenced by the mass-load introduced by the SiO_2 layer. Hence a variation in the thickness of either layer will affect both the fundamental modes and their harmonics. The quality factors at the series (Q_s) and parallel (Q_p) resonant frequencies and the effective electromechanical coupling factor (k_{eff}^2) were derived from the IEEE standard definitions (IEEE standard on 1987)

$$Q = \frac{1}{2} f_r \frac{\partial \varphi}{\partial f} \quad (1)$$

$$k_{\text{eff}}^2 = \frac{\pi f_r}{2 f_a} \frac{1}{\tan\left(\frac{\pi f_r}{2 f_a}\right)} \quad (2)$$

where φ represents the admittance phase and f_a represents the anti-resonance frequency. Q_p was found to be 1380 and 840 for

Download English Version:

<https://daneshyari.com/en/article/867317>

Download Persian Version:

<https://daneshyari.com/article/867317>

[Daneshyari.com](https://daneshyari.com)